Anal. Chem. **2010,** *82,* 1546–1550

Spinning Disk Platform for Microfluidic Digital Polymerase Chain Reaction

Scott O. Sundberg,* Carl T. Wittwer, Chao Gao, and Bruce K. Gale

University of Utah, Rm 5R441, 1795 E South Campus Dr., Salt Lake City, Utah 84112

An inexpensive plastic disk disposable was designed for digital polymerase chain reaction (PCR) applications with a microfluidic architecture that passively compartmentalizes a sample into 1000 nanoliter-sized wells by centrifugation. Well volumes of 33 nL were attained with a 16% volume coefficient of variation (CV). A rapid air thermocycler with aggregate real-time fluorescence detection was used, achieving PCR cycle times of 33 s and 94% PCR efficiency, with a melting curve to validate product specificity. A CCD camera acquired a fluorescent image of the disk following PCR, and the well intensity frequency distribution and Poisson distribution statistics were used to count the positive wells on the disk to determine the number of template molecules amplified. A 300 bp plasmid DNA product was amplified within the disk and analyzed in 50 min with 58−1000 wells containing plasmid template. Target concentrations measured by the spinning disk platform were 3 times less than that predicted by absorbance measurements. The spinning disk platform reduces disposable cost, instrument complexity, and thermocycling time compared to other current digital PCR platforms.

Digital polymerase chain reaction (PCR) is a highly sensitive DNA and RNA quantification technique that counts each template individually. This technique provides greater precision over quantitative real-time PCR (qPCR) because it is not sensitive to PCR efficiency, transforming exponential, analog signals to linear, digital signals.[1] First published in 1999, limiting dilution was used to detect a minor fraction of altered DNA by diluting to the point of having 0.5 DNA templates per PCR in a microtiter plate format.[2] Molecular beacon probes were analyzed following PCR to quantify the wild type to rare mutation ratio, relying on binary positive/negative calls.

More recently, the concept of digital PCR has been miniaturized to nanoliter volumes using microfluidics to limit the amount of DNA template in a PCR.[3] Miniaturization of PCR volume has benefited digital PCR in three significant ways. First, reagent consumption is reduced 100 to 1000-fold from microtiter plate formats, reducing testing costs dramatically. Second, the number of parallel reactions has increased over 100-fold, thus increasing power, sensitivity, and throughput. Third, testing is simplified by reducing sample dilution steps, using volume as a limiting factor, and eliminating several pipetting steps required with microtiter plates. Miniaturization of digital PCR has been investigated down to 65 pL reaction volumes.[4]

Applications of microfluidic digital PCR include detection of rare mutations within an excess of normal DNA,[5] multigene analysis of bacteria,[6] copy number variation,[7] fetal DNA in maternal plasma,[8] and genetic allelic imbalance.[9,10]

The purpose of this work is to improve upon current microfluidic digital PCR platforms by reducing disposable costs, instrument complexity, and time to result. Our design loads the sample into nanoliter-sized compartments by centrifugation, eliminating the need for valves and pumps and reducing microfluidic loading time. The disk consists of three inexpensive plastic thin film sheets laminated together with an architecture that passively divides a spun sample into a thousand compartments, reducing chip disposable costs. PCR is performed on the rotating disk by rapid thermal cycling in an air chamber, reducing thermocycling time. After PCR, each compartment is interrogated for a positive/negative signal by fluorescence imaging.

In this work, we demonstrate microfluidic digital PCR within a spinning disk platform in less than 35 min (including disk loading, PCR thermocycling, and fluorescent imaging). A single disk provides 1000 nanoliter-sized reactions detected with the dsDNA fluorescent saturating dye LCGreen.[11] No labeled probes are required.

MATERIALS AND METHODS

Disk Design and Manufacturing. The disk design is based on the use of centrifugal force to move fluid along a spiral channel, filling wells along the way. A loading reservoir located near the center of the disk is connected to a spiral channel, 250 μm wide,

* To whom correspondence should be addressed. E-mail: scott.sundberg@m.cc.utah.edu.

(1) Pohl, G.; Shih, Ie. M. *Expert Rev. Mol. Diagn.* **2004**, *4*, 41–47.
(2) Vogelstein, B.; Kinzler, K. W. *Proc. Natl. Acad. Sci. U.S.A.* **1999**, *96*, 9236–9241.
(3) Warren, L.; Bryder, D.; Weissman, I. L.; Quake, S. R. *Proc. Natl. Acad. Sci. U.S.A.* **2006**, *103*, 17807–17812.
(4) Kiss, M. M.; Ortoleva-Donnelly, L.; Beer, N. R.; Warner, J.; Bailey, C. G.; Colston, B. W.; Rothberg, J. M.; Link, D. R.; Leamon, J. H. *Anal. Chem.* **2008**, *80*, 8975–8981.
(5) Yung, T. K. F.; Chan, K. C. A.; Mok, T. S. K.; Tong, J.; To, K.-F.; Lo, Y. M. D. *Clin. Cancer Res.* **2009**, *15*, 2076–2084.
(6) Ottesen, E. A.; Hong, J. W.; Quake, S. R.; Leadbetter, J. R. *Science* **2006**, *314*, 1464–1467.
(7) Qin, J.; Jones, R. C.; Ramakrishnan, R. *Nucleic Acids Res.* **2008**, *36*, e116.
(8) Lun, F. M. F.; Chiu, R. W. K.; Chan, K. C. A.; Leung, T. Y.; Lau, T. K.; Lo, Y. M. D. *Clin. Chem.* **2008**, *54*, 1664–1672.
(9) Fan, H. C.; Quake, S. R. *Anal. Chem.* **2007**, *79*, 7576–7579.
(10) Fan, H. C.; Blumenfeld, Y. J.; El-Sayed, Y. Y.; Chueh, J.; Quake, S. R. *Am. J. Obstet. Gynecol.* **2009**, *200*, 543.e1543.e7.
(11) Wittwer, C. T.; Reed, G. H.; Gundry, C. N.; Vandersteen, J. G.; Pryor, R. J. *Clin. Chem.* **2003**, *49*, 853–860.

10.1021/ac902398c
Published on Web 01/19/2010

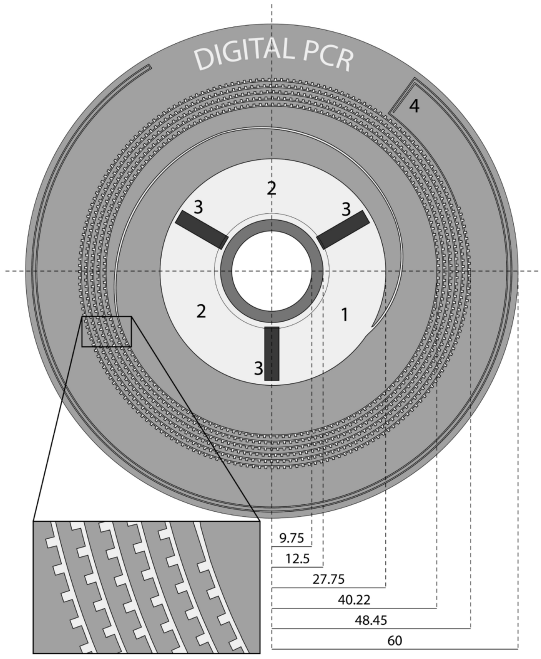

Figure 1. Spinning disk design, with dimensions given in millimeters, shown to scale. The disk consists of a loading reservoir, spiral microchannel with 1000 wells facing radially outward along the channel, and an overflow channel at the edge of the disk. The PCR mixture is pipetted into the loading reservoir at location 1, and mineral oil is pipetted into the loading reservoir at location 2. The Teflon inserts for the loading reservoir are also shown (3). A pin-sized hole is located at the end of the overflow channel (4), and once the disk is loaded, this same location is thermally sealed, creating a closed system for PCR.

that moves toward the outside of the disk. Along the channel are square wells, facing radially outward along the spiral, which are designed as fluid traps. This design is fabricated from thin film plastics to create an inexpensive disposable, requiring only centrifugation for fluid control. The current design consists of 1000 wells each having dimensions of 500 μm × 500 μm × 125 μm. The entire disk is 120 mm in diameter, the size of a CD, and is 375 μm thick. The channel layer disks were manufactured using the process of xurography.[12,13] Figure 1 illustrates the disk design (see Supporting Information for more details).

Sample Preparation. We evaluated the feasibility of digital PCR within the spinning disk using a previously developed DNA "Toolbox".[14] Plasmid from the DNA Toolbox was provided by Lonza (Rockland, ME). The PCR mixture contained plasmid DNA, ranging from 6×10^6 to 6×10^0 copies/μL (determined by absorbance) as the template. Preparation details of the plasmid DNA and PCR mixture can be found in the Supporting Information.

Disk Loading. The sample was loaded by pipetting 40 μL of PCR mix and 250 μL of mineral oil (M5904, Sigma-Aldrich Corporation), dyed with Oil Red O (Matheson Coleman & Bell, Gardena, CA), into the loading reservoir of the disk. Two polycarbonate disks, 750 μm thick with an outer diameter of 75 mm, were then coupled to each side of the disk, using a two-piece collar, to provide more rigidity to the disk during thermocycling. The disk was then spun at 4000 rpm for 5 min to move the fluid from the middle to the outside of the disk, filling each of the wells along the way and leaving the channel filled with the mineral oil, as seen in Figure S1 in the Supporting Information. The end of the spiral channel was then thermally sealed prior to thermocycling to create a closed system. The collar was attached to the servo motor shaft within the thermocycler using a set screw.

Thermocycling. A previously described rapid air thermocycling instrument[15] was modified to spin the disk at controllable speeds, measure disk temperature during thermocycling, and measure the average fluorescence of disk wells, as seen in Figure S2 (see Supporting Information for more details). Forty-five cycles of 45 °C annealing for 0 s, 72 °C extension for 2 s, and 90 °C denaturing for 0 s was achieved in under 25 min while spinning the disk at 2500 rpm (33 s/cycle).

A fluorimeter was mounted to the thermocycler with an excitation spot size of 1 mm in diameter aimed 45 mm from the center of the disk, providing an average real-time fluorescence reading over hundreds of wells due to the disk spinning during fluorescence acquisition (see Supporting Information for details). The fluorimeter optics scheme is shown in Figure S3. The real-time fluorescence data at PCR extension was normalized, multiplying the extension fluorescence value by the difference between the annealing and denaturing fluorescence values at each cycle. The quantification cycle (C_q) for each test was determined by inputting these normalized fluorescence values into LightCycler Software vs 3 (Roche Diagnostics, Indianapolis, IN). The melting temperature (T_m) of the amplified product was also determined by LightCycler software, inputting the temperature and fluorescence data for the last thermocycle between 70 and 90 °C. The T_m is defined as the maxima of the negative first derivative of fluorescence.[16] The fluorescent signal is sufficient to obtain melting curves even within nanoliter volumes.[17]

Disk Imaging and Analysis. The disk was fluorescently imaged following PCR for digital well analysis, with the imaging setup seen in Figure S4 (see Supporting Information for more details). ImageJ[18] software was used to threshold, size exclude, and then create histograms of well intensity for each disk image. The threshold and minimum pixel number was operator defined. Histogram frequency distributions were then used to determine the number of positive and negative wells for each test.

Measuring Well Volume Variation. PCR amplicon with dsDNA fluorescent dye and mineral oil were spun into the disk to determine well volume variation. A fluorescent image of the disk was taken. The number of pixels of each well along with the mean and standard deviation of well fluorescence was obtained using custom LabView software. The pixels were used to calculate the surface area of fluid within each well. This surface area was then multiplied by the depth of the well, which is the thickness of the middle layer of plastic, to determine well volume. A nonfluorescent imaging method was also used to determine well

(12) Bartholomeusz, D. A.; Bouttè, R.; Andrade, J. D. *J. Microelectromech. Syst.* **2005**, *14*, 1364–1374.
(13) Greer, J.; Sundberg, S. O.; Wittwer, C. T.; Gale, B. K. *J. Micromech. Microeng.* **2007**, *17*, 2407–2413.
(14) Highsmith, W., Jr.; Jin, Q.; Nataraj, A.; O'Connor, J.; Burland, V.; Baubonis, W.; Curtis, F.; Kusukawa, N.; Garner, M. *Electrophoresis* **1999**, *20*, 1186–94.
(15) Wittwer, C. T.; Ririe, K. M.; Andrew, R. V.; David, D. A.; Gundry, R. A.; Balis, U. J. *Biotechniques* **1997**, *22*, 176–181.
(16) Ririe, K. M.; Rasmussen, R. P.; Wittwer, C. T. *Anal. Biochem.* **1997**, *245*, 154–160.
(17) Sundberg, S. O.; Wittwer, C. T.; Greer, J.; Pryor, R. J.; Elenitoba-Johnson, O.; Gale, B. K. *Biomed. Microdevices* **2007**, *9*, 159–166.
(18) Rasband, W. S. U.S. National Institutes of Health, Bethesda, Maryland, http://rsb.info.nih.gov/ij/ 1997–2009 (Accessed June 8, 2009).

manufacturing variation. Well dimensions were determined by measuring the edges of 5% of the wells to calculate the surface area, using pixels to determine edge lengths, and then multiplying the surface area by well depth for manufactured well volume variation.

RESULTS AND DISCUSSION

The spinning disk platform performed digital PCR with rapid PCR thermocycling using only a dsDNA fluorescent saturating dye, providing quantification results within 50 min. Thermocycle times (33 s cycles) were much faster than some reported platforms (~120 s cycles[3] and 55 s cycles[4]). The disk disposable was inexpensive and easy to load, requiring less than 5 min. Fluorescent imaging of the disk required an additional 5 min. Image analysis required 15 min for positive well quantification but could be streamlined in future software. Microfluidics allows digital PCR to use much less reagent than microtiter plate systems, and the absence of labeled probes further reduced costs by simply using a dsDNA fluorescent saturating dye.

Well Volume Variation. PCR amplicon with dsDNA dye and mineral oil were spun into the disk to determine well volume variation. The wells had a mean volume of 33 nL with a standard deviation of ±5.2 nL or a 16% volume CV, across all 1000 wells. It was further found that the manufacturing method alone causes a 10% volume CV due to variation in well cutting from the cutting plotter based on cut well dimensions.

Dilution Series. A dilution series was performed using the spinning disk platform to determine PCR efficiency and to identify the concentrations required for optimal digital PCR results. The dilution series ranged from 6×10^6 to 6×10^0 plasmid copies/μL, or about 200 000 to 0.2 plasmid copies/well. An example of the unprocessed real-time data is shown in Figure 2 for the highest plasmid concentration of 6×10^6 plasmid copies/μL. Figure S5 in the Supporting Information shows the real-time PCR curves for each dilution. Table 1 provides the C_qs, T_ms, and number of positive wells for each plasmid concentration run in the spinning disk platform. A PCR efficiency of 94% was calculated, using the 6×10^6 to 6×10^2 C_q data and excluding the last two concentrations because they were in the "digital range", from the equation

$$\text{PCR efficiency} = 10^{-1/\text{slope}} - 1 \qquad (1)$$

where the slope is found when the logarithm of template concentration is plotted on the x axis and C_q is plotted on the y axis. The slope was −3.47 with a correlation coefficient, R^2 value, of 0.989 for the dilution series. Figure 3 shows fluorescent images of the disk for the four lowest concentrations in the dilution series. A histogram for the concentration of 6×10^1 plasmid copies/μL is also shown in Figure 3 to illustrate the frequency distributions that were used to determine the number of positive wells within each disk. The PCR product T_ms had a mean temperature of 84.4 °C and a standard deviation of 0.7 °C. The T_m helps validate PCR product specificity.

The digital PCR concentrations, 6×10^1 and 6×10^0 plasmid copies/μL, had 518 and 58 positive wells, respectively. Because the plasmid is homogeneously mixed within the PCR, a Poisson distribution is assumed to statistically determine the number of plasmid copies present for each disk. As the number of positive wells increases, the chance of having more than one copy of DNA in a given positive well also increases. The Poisson distribution follows the equation

$$f(x) = (\lambda^x) \times (e^{-\lambda}) / (x!) \qquad (2)$$

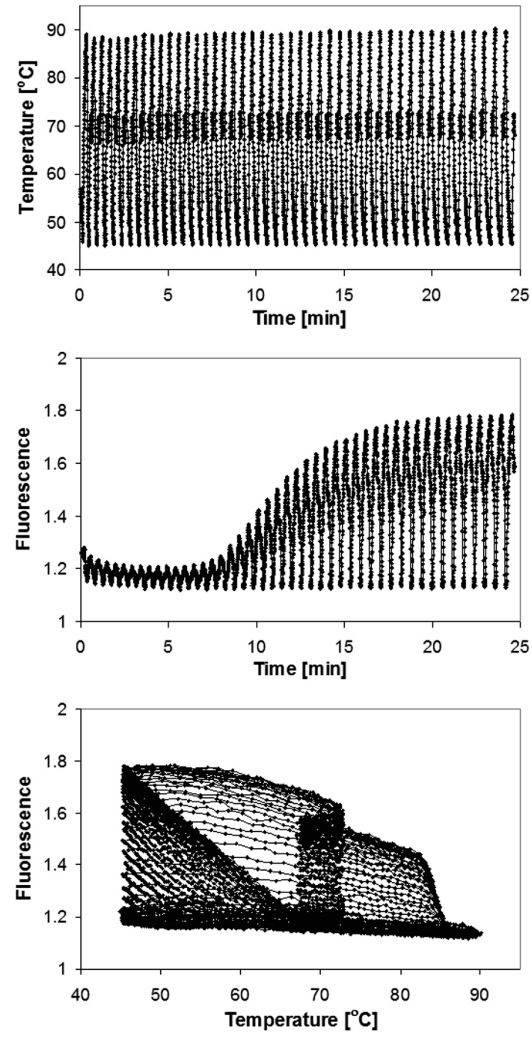

Figure 2. Real-time plots are shown of temperature vs time (top), fluorescence vs time (middle), and fluorescence vs temperature (bottom) at a concentration of 6×10^6 plasmid copies/μL. The top plot illustrates that 45 thermocycles required less than 25 min; the middle plot shows the exponential increase in fluorescence with a C_q of 16, and the bottom plot provides the T_m of the amplified product, seen at 84.6 °C.

Table 1. Quantification Cycle (C_q), Melting Temperature (T_m), and Number of Positive Wells for Template Dilution on the Spinning PCR Disk

conc. [copies/μL]	C_q [cycle no.]	T_m [°C]	positive wells
6×10^6	16	84.6	997
6×10^5	19.57	85.3	992
6×10^4	24.05	84.6	974
6×10^3	27.13	84.5	995
6×10^2	29.57	83.1	939
6×10^1	32.02	84.1	518
6×10^0	32.28	*a*	58

[a] Signal was too low to detect the melting transition at this concentration.

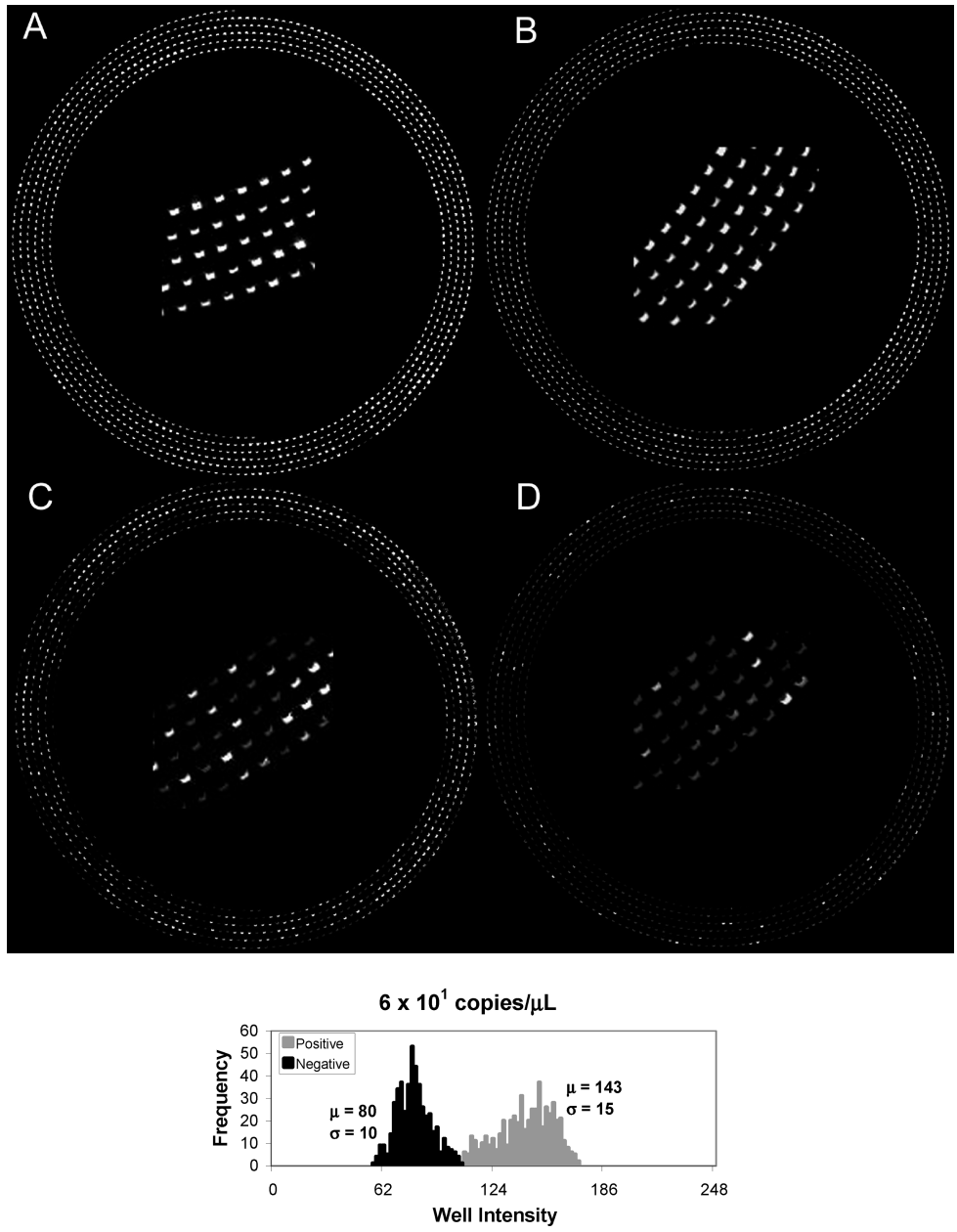

Figure 3. (Top) Fluorescent images are presented for 6×10^3 plasmid copies/μL (A), 6×10^2 plasmid copies/μL (B), 6×10^1 plasmid copies/μL (C), and 6×10^0 plasmid copies/μL (D). A lower right section of each disk image is enlarged. Digital PCR is achieved with dilutions C and D, where image C has 518 and image D has 58 out of 1000 wells fluorescing. (Bottom) An example of the histogram data used to determine the number of positive wells is shown for the 6×10^1 plasmid copies/μL concentration.

where λ is the mean number of template copies and x is the number of templates of interest present for a given well. If 48.2% of the wells are empty, as is the case with the 6×10^1 plasmid copies/μL disk, then the expected number of copies per well is $-\ln 0.482$ or 0.730 (which is the λ value solved when $f(0) = 0.482$ and $x = 0$). Therefore, although 518 positive wells are present, there are ~730 plasmid copies that have actually been amplified. A similar calculation is made for the 6×10^0 plasmid copies/μL disk in which the expected number of copies per well is 0.060; in other words, ~60 plasmid copies were amplified although 58 positive wells were counted.

A discrepancy exists between the absorbance measurements of the plasmid and the digital results found in the two lowest concentrations. At 6×10^1 plasmid copies/μL, there should be 2 copies/well although only 0.730 copies per well was measured, and at 6×10^0 plasmid copies/μL, there should be 0.2 plasmid copies/well although only 0.060 plasmid copies/well was measured. This means that the spinning disk platform differs from absorbance measurements by about a factor of 3. The plasmid purity is unknown and may account for some of the discrepancy. There may also be a portion of the plasmid not cleaved or linearized that delays PCR amplification. Another possibility is that some of the plasmid may adsorb to the plastic as it moves through the loading reservoir and spiral microchannel. The addition of PVP to the PCR mix diminishes these effects greatly but may not entirely resolve the issue. This is apparent in the three lowest concentrations where the first several wells do not fluoresce, possibly caused by plasmid adsorbing to the plastic in the frontrunner fluid and then filling those first wells without template.

Not all wells fluoresced with the positive controls. Some of this stems from the cutting plotter which occasionally creates undesirable ridges next to a well, causing irregular fluid flow and allowing mineral oil to fill the well rather than the PCR mix. The other issue is that the disk manufacturing did not take place in a clean room, and therefore, an occasional dust particle was present in a well, disrupting adequate PCR amplification.

CONCLUSION

Plasmid DNA was efficiently PCR amplified within the spinning disk platform and analyzed in 50 min with 58−1000 wells containing template. Subsequent work will focus on improving the plastic disk manufacturing, eliminating DNA adsorption to the disk, reducing analysis time, designing a rapid air cycler fitted to the disk for faster thermocycling, and investigating new digital PCR applications. A fluorescent scanner for the disk is also envisioned to replace disk imaging following PCR to provide higher "on/off" fluorescence resolution and further reduce instrumentation cost.

ACKNOWLEDGMENT

The authors thank the University of Utah Research Foundation for kindly supporting this work. We also thank Dr. Wittwer's lab group and Dr. Gale's lab group for valuable advice pertaining to this research.

SUPPORTING INFORMATION AVAILABLE

Additional information as noted in text. This material is available free of charge via the Internet at http://pubs.acs.org.

Received for review October 22, 2009. Accepted December 31, 2009.

AC902398C